FI SEVIER

Contents lists available at ScienceDirect

Journal of Molecular and Cellular Cardiology

journal homepage: www.elsevier.com/locate/yjmcc



Original article

PARP mediates structural alterations in diabetic cardiomyopathy

Jane Chiu, Hana Farhangkhoee, Bing Ying Xu¹, Shali Chen, Biju George, Subrata Chakrabarti*

Department of Pathology, 4033 Dental Sciences Building, University of Western Ontario, London, Ontario, Canada

ARTICLE INFO

Article history:
Received 28 April 2008
Received in revised form 16 June 2008
Accepted 24 June 2008
Available online 8 July 2008

Keywords: Diabetic cardiomyopathy Hyperhexosemia PARP p300

ABSTRACT

Diabetic cardiomyopathy is characterized by structural alterations such as cardiomyocyte hypertrophy, necrosis and focal fibrosis. Hyperglycemia-induced oxidative damage may play an important role in this pathogenetic process. Recent studies have shown that poly (ADP-ribose) polymerase (PARP) is activated in response to oxidative stress and cellular damage as well, plays a role in gene expression. This study investigated mechanisms of diabetes-induced, PARP-mediated development of structural alterations in the heart. Two models of diabetic complications were used to determine the role of PARP in oxidative stress, cardiac hypertrophy and fibrosis in the heart, PARP-1 knockout (PARP-/-) mice and their respective controls were fed a 30% galactose diet while male Sprague-Dawley rats were injected with streptozotocin and subsequently treated with PARP inhibitor 3-aminobenzamide (ABA). The in vivo experiments were verified in in vitro models which utilized both neonatal cardiomyocytes and endothelial cells. Our results indicate that hyperhexosemia caused upregulation of extracellular matrix proteins in association with increased transcriptional co-activator p300 levels, cardiomyocyte hypertrophy and increased oxidative stress. These pathogenetic changes were not observed in the PARP^{-/-} mice and diabetic rats treated with ABA. Furthermore, these changes appear to be influenced by histone deacetylases. Similar results were obtained in isolated cardiomyocytes and endothelial cells. This study has elucidated for the first time a PARP-dependent, p300-associated pathway mediating the development of structural alterations in the diabetic heart.

© 2008 Elsevier Inc. All rights reserved.

1. Introduction

Pathogenetic mechanisms leading to the development of diabetic cardiomyopathy may involve both endothelial cells and cardiomyocytes. Structurally, diabetic cardiomyopathy is characterized by capillary basement membrane thickening and focal fibrosis due to increased production of extracellular matrix (ECM) proteins and cardiomyocyte hypertrophy [1,2]. Increased oxidative stress from chronic hyperglycemia may play a significant role in this process. Oxidative stress leads to DNA breakage which renders the DNA unstable thereby activating nuclear enzyme poly (ADP-ribose) polymerase (PARP) in an attempt to repair such damage. Activated PARP transfers ADP-ribose units from NAD+ (nicotinamide adenine dinucleotide) to itself and other nuclear chromatin-associated proteins [3]. When PARP is overactivated, which is the case in diabetes, intracellular NAD+ is depleted creating a redox imbalance further exacerbating the oxidative state in the cell. The beneficial effects of PARP inhibition has been illustrated by PARP-1 knockout (PARP^{-/-}) mice. These animals are protected against streptozotocin (STZ)induced diabetes [4] and myocardial ischemia/reperfusion injury [5] among other diseases.

Transcriptional co-activator and histone acetyltransferase (HAT) p300 mediates cell growth, proliferation and differentiation as well, it controls a large number of transcription factors, nuclear receptors and DNA repair enzymes including PARP [6,7]. PARP itself has been shown to facilitate p300-mediated gene transcription [8]. Previously, we have shown that diabetes upregulates the expression of p300 along with PARP activity and that inhibition of p300 prevents diabetes-induced upregulation of PARP mRNA and ECM protein fibronectin (FN). FN plays a variety of physiological roles including cell survival, migration and proliferation [9]. We have also shown that in diabetes, increased ECM protein production may be mediated through the activation of vasoactive factors such as endothelin-1 (ET-1) [10,11]. It is however not clear as to the role of PARP and its relationship with epigenetic mechanisms, such as p300 activation, in the pathogenesis of diabetic cardiomyopathy.

The role of PARP activation has been demonstrated to alter the function of the heart in diabetes. However, PARP has not been studied with respect to structural changes in the diabetic heart. Hence, in this study we investigated the role of PARP in the development of structural alterations in the heart in diabetes. We determined whether these effects were mediated in association with p300 in PARP-/- animals fed a 30% galactose diet as well as chemically-induced diabetic animals. Galactose-fed animals are well studied as a model of chronic diabetic complications with both biochemical and structural changes of chronic diabetic complications having been shown in this model [12,13]. These animals also exhibit diabetes-like contractile

^{*} Corresponding author. Tel.: +1 519 685 8500x36350; fax: +1 519 661 3370. E-mail address: Subrata.Chakrabarti@schulich.uwo.ca (S. Chakrabarti).

 $^{^{\}rm 1}$ Current address: Department of Forensic Science, Kunming Medical College, Kunming, Yunnan, P.R. China.

abnormalities in the heart [14]. We further used a well-studied streptozotocin-induced diabetic rat model [11,14] as well as neonatal rat cardiomyocytes and endothelial cells to study mechanistic pathways [10].

2. Research design and methods

2.1. Animal models

All animals were cared for according to the Guiding Principle in the Care and Use of Animals. All experiments were approved by the University of Western Ontario Council on Animal Care Committee.

PARP^{-/-} and wild type (WT) littermates (129S/SvImJ) were purchased from Jackson Laboratories (ME, USA). At 6 weeks of age, males from both PARP^{-/-} and WT groups were randomly divided into two groups. The mice were given either a standard rodent diet (CO) containing 19% protein, 5% fat and 5% crude fiber or a similar feed enriched with 30% galactose (*G*, Test Diet, IN, USA). These animals were maintained for a period of 8 weeks.

Male Sprague–Dawley rats weighing 200–250 g were purchased from Charles River (QC, Canada) and randomly divided into 3 groups: control (CO), diabetic (DM) or diabetic treated with PARP inhibitor 3-aminobenzamide (DM-ABA, MP Biomedical, Inc, OH, USA). Diabetes was induced by a single intravenous injection of STZ (65 mg/kg in citrate buffer, pH=5.6), while the control animals were injected with the same volume of citrate buffer. ABA, reconstituted in saline, was administered (30 mg/kg/day [15]) intraperitoneally for a period of 4 months. The control animals received saline injections of a similar volume. These animals were monitored daily and implanted with insulin implants that released small doses of insulin to prevent ketonuria (2 U/day, Linshin Canada Inc, ON, Canada).

Clinical monitoring of both groups of animals was performed through regular assessment of body weight and blood reducing sugar levels. The animals were sacrificed and the hearts were excised and weighed. Two mm thick portions of cardiac tissue was removed 2 mm above the apex and fixed in 10% formalin for immunohistochemical analysis. The remainder of the tissue was snap frozen.

2.2. RNA extraction and real time RT-PCR analysis

RNA was isolated from mice and rat heart tissues as well as from human umbilical endothelial vein (HUVECs; see below) as previously described [10]. cDNA was synthesized from the total RNA. The mRNA levels of FN, ET-1, p300 and heme oxygenase (HO-1) were quantified using LightCycler™ (Roche Diagnostics Canada, QC, Canada). The data was normalized to housekeeping gene 18S rRNA to account for reverse transcription efficiencies. The primer sequences for mouse ET-1 are: 5′-TTAGCAAGACCATCTGTGTG-3′ and 5′-GAGTTTCTCCCTGAAATGTG-3′. The primer sequences for mouse p300 are: 5′-AGGCAGAGTAGGA-CAGTGAA-3′ and 5′-CTCAGTCTGGGTCACTCAAT-3′. The primer sequences for mouse HO-1 are: 5′-TGAACACTCTGGAGATGACA-3′ and 5′-AACAGGAAGCTGAGAGTGAG-3′. All other primer sequences have previously been described [16,17].

2.3. Histological analysis

Formalin fixed tissues were embedded in paraffin, sectioned at 5 µM thickness and placed on positively charged slides. Trichrome staining was performed to assess ECM protein deposition and fibrosis.

The heart tissues were also analyzed for 8-hydroxy-2'-deoxyguanosine (8-OHdG, Chemicon International, Inc, CA, USA), a sensitive marker for oxidative DNA damage [18] and nitrotyrosine (NT, Cayman Chemical Company, MI, USA), a marker for oxidative protein damage [19]. The slides were stained using Vectastain Elite (Vector Laboratories Canada, Inc, ON, Canada) for 8-OHdG and EnVision (Dako Canada, Inc, ON, Canada) for NT as each reagent recognized a different

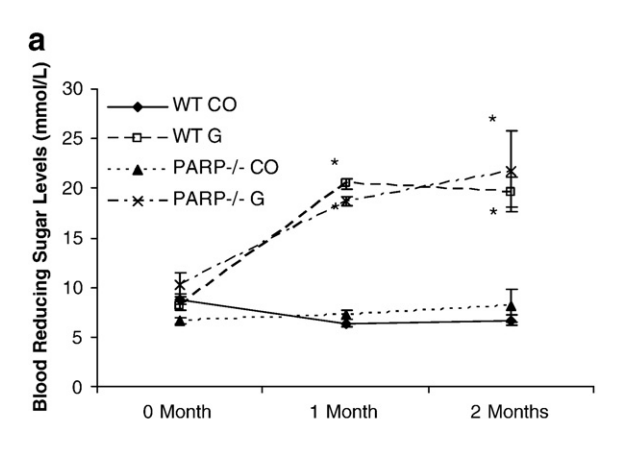
host. The chromagen 3,3′ diaminobenzine (DAB, Sigma-Aldrich, ON, Canada) was used for detection. Ten random fields were examined by two investigators unaware of the experimental treatment. 8-OHdG immunoreactivity was assessed by the presence of positively stained nuclei while NT was evaluated by comparing the relative staining intensity in the cytoplasm.

2.4. Catalase activity assay

Catalase activity was assessed in the mice hearts using a commercially available colorimetric kit (E-100, Biomedical Research Service Center University at Buffalo, NY, USA). This kit is based on the premise that the presence of catalase reduces the amount of $\rm H_2O_2$ and thus inhibits the oxidation of the chromagen. Total protein was extracted and quantified. Five $\rm \mu g$ of protein was used in each assay as per manufacturer's instructions. Catalase activity is expressed as optical density at 410 nm.

2.5. Immunofluorescence

PARP activation in the rat hearts was determined using a monoclonal mouse antibody (1:200, Biomol International L.P., PA, USA). In addition, neonatal cardiomyocytes were fixed in methanol and stained with a mouse monoclonal phospho-H2A.X antibody (1:200, Abcam, Inc, MA, USA) to assess double stranded DNA breaks [20]. An Alexa Fluor® 488-labelled anti-mouse secondary antibody (Invitrogen Canada, Inc, ON, Canada) was used for detection using a fluorescent microscope (Olympus BX51, Olympus Canada Inc, ON, Canada) and Northern Eclipse software (Empix Inc, ON, Canada).



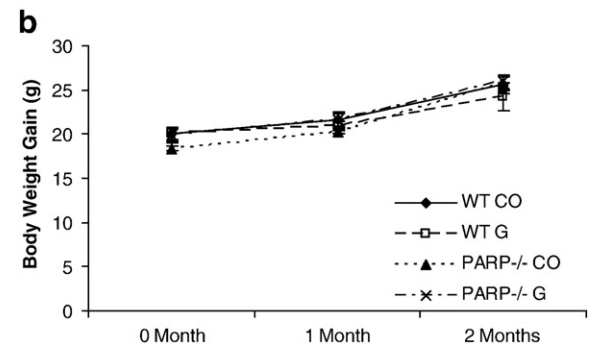


Fig. 1. Clinical monitoring of the mice showing significantly increased blood reducing sugar levels in the galactosemic animals compared to the control animals (a) and no significant differences in body weight gain during the course of the experiment between all groups (b). PARP gene ablation had no effect on these parameters $[n=5; WT=wild type, PARP^{-/-}=PARP-1 knockout, CO=control, G=30% galactose diet; <math>*p < 0.05$ compared to controls].

Hoechst 33342 dye (1 μ g/mL, Invitrogen Canada Inc, ON, Canada) was used to visualize the nuclei.

2.6. Histone deacetylase (HDAC) activity assay

Nuclear protein extracts were prepared from heart tissues (50–100 mg) of both rats and mice as previously described [21]. HDAC activity from 100 μ g of nuclear extract was determined using the HDAC activity assay kit (ab1432, AbCam Inc, MA, USA) as per manufacturer's instructions. HDAC activity is expressed as the absolute amount of deacetylated lysine generated in each sample (μ mol/L).

2.7. Cardiomyocyte isolation and culture

Myocytes were prepared from 1 to 2 day old neonatal Sprague-Dawley rat heart ventricles as previously described [22,23]. Nonmyocytes were removed through differential attachment. The isolated cardiomyocytes were then plated onto 6 well culture plates (PrimariaTM Falcon, NJ, USA) at a density of 3.0×10^4 cells/cm². The cells were maintained for 48 h in Dulbecco's Modified Eagle's Medium/Ham's F-12 supplemented with 10% fetal bovine serum, 10 µg/mL transferrin selenium, 10 µg/mL insulin, 10 ng/mL selenium, 50 U/mL penicillin, 50 µg/mL streptomycin, 2 mg/mL bovine serum albumin, 5 µg/mL linoleic acid, 3 mN pyruvic acid, 0.1 mmol/L minimum essential medium (MEM) non-essential amino acids, 10% MEM vitamin, 0.1 mmol/L bromodeoxyuridin, 100 μm L-ascorbic acid, and 30 mmol/L HEPES (pH 7.1). The cells were serum-starved overnight and treated with either 5 mmol/L of PARP inhibitor ABA or 16 µmol/L of 1,5-isoquinolinediol (ISO, Sigma-Aldrich, ON, Canada) for 1 h. The cardiomyocytes were then subjected to either a 5 mmol/L glucose (low glucose, LG) or a 25 mmol/L glucose (high glucose, HG) environment for 24 h. LG was used as controls.

2.8. Endothelial cell culture

HUVECs (Clonetics, MD, USA) were cultured in endothelial cell growth medium (Clonetics, MD, USA). The cells were serum-starved overnight and exposed to either 5 mmol/L of PARP inhibitor ABA dissolved in ddH₂0 or 0.01 μmol/L of HDAC inhibitor trichostatin A (TSA, Calbiochem, NJ, USA) dissolved in DMSO for 1 h. The cells were then incubated with 5 mmol/L of p-glucose or 25 mmol/L of glucose and maintained for 24 h. We have previously determined that these concentrations of glucose are optimal for studying glucose-induced gene expression alterations [10,17]. Twenty five mmol/L of L-glucose were used as controls (data not shown). The endothelial cells were subsequently used for RNA extraction and cDNA synthesis for RT-PCR analyses (see above). HUVECs treated with TSA are normalized to RPL13A as the mRNA level of this housekeeping gene has been shown to remain the most constant with TSA treatment [24].

2.9. Measurement of cardiomyocyte hypertrophy

Cell surface area of cardiomyocytes was measured to assess cellular hypertrophy. The cells were visualized using a Leica DMIL inverted microscrope (Leica Wetzlar, Germany) equipped with a Polaroid digital camera. The images were captured at 10× magnification. Cell surface area was determined using Mocha™ Software (SPSS, IL, USA) from 50 randomly selected cells per experiment, then averaged and expressed as pixels.

2.10. Statistical analysis

The data is expressed as mean±SEM. Statistical significance was determined by ANOVA followed by Bonferroni/Dunn test. Differences were considered to be statistically significant at values of p < 0.05.

3. Results

3.1. Hyperhexosemia-induced PARP activation and increased oxidative stress is prevented with PARP inhibition

Both mice and rats were monitored for diabetic dysmetabolism by evaluating body weight gain and blood reducing sugar levels. Galactose-fed diabetic mice showed significant elevation of blood reducing sugar levels after one and two months of galactose feeding, however, no significant reduction of body weight was observed. No effect of PARP^{-/-} was seen on blood sugar levels or body weight. These data are shown in Figs. 1a and b, respectively. The diabetic rats showed significantly reduced body weight (484.0±40.3 g vs. 613.5±13.8 g in controls) and hyperglycemia (18.4±6.8 mmol/L vs. 7.22±1.6 mmol/L) after 4 months of follow up. PARP inhibition had no significant effect on these parameters (526.1±17.9 g and 22.6±4.7 mmol/L).

We first determined whether diabetes does in fact increase the activation of PARP in the heart. Rat heart sections were immunofluor-escently assessed for PARP activation using a monoclonal PARP antibody. In the diabetic animals, there was increased nuclear positivity for PARP compared to the control counterparts (Fig. 2a). PARP inhibition with ABA treatment prevented this diabetes-induced effect.

Next we assessed hyperhexosemia-induced oxidative damage in the heart. A catalase activity assay was performed on the mice. The WT galactose-fed mice exhibited significantly increased activity compared to the WT control animals. It is of interest to note that the PARP^{-/-} control mice had significantly lower levels of catalase compared to the WT controls. The galactose-fed PARP^{-/-} mice had catalase levels similar to the controls (Fig. 2b). These data were further verified with immunohistochemistry using two markers of oxidative damage. The WT mice fed a galactose rich diet showed increased nuclear staining of 8-OHdG, a marker of oxidative DNA damage compared to the WT control mice (Fig. 2c). This was paralleled in the rats, where the STZ-induced diabetic rat hearts exhibited increased nuclear staining of 8-OHdG, compared to their age-matched controls (Fig. 2d). Interestingly, the galactose-fed PARP^{-/-} mice and the diabetic rats treated with ABA showed complete normalization of the hyperhexosemia-induced effects (Figs. 2c and d).

We then tested the effect of PARP inhibition on oxidative stress by using another sensitive oxidant injury marker. Analysis of the WT mice on the high galactose diet with NT, a marker of oxidative protein damage, showed increased staining intensity in the cytoplasm compared with the hearts of the WT animals on normal diet (Fig. 2c). A similar pattern was also seen in the diabetic rat hearts (Fig. 2d). Cardiac tissue from the galactose-fed PARP^{-/-} mice and the diabetic rats with ABA treatment showed a NT staining pattern that is reminiscent of their respective control hearts; again indicating complete attenuation of the hyperhexosemia-induced effects (Figs. 2c and d). These results were further confirmed by the analysis of a prooxidant marker HO-1 [25] transcript levels. Cardiac tissues of WT galactose-fed mice showed a significant upregulation of HO-1 (data not shown). Inhibition of PARP also prevented this hyperhexosemia associated increase in the mice (data not shown). These findings are in support of Garcia Soriano et al. who found that PARP activation increased NT positivity in the blood vessels of diabetic mice and that pharmacological PARP inhibition can prevent this diabetes-induced effect [26].

3.2. Hyperhexosemia-induced ECM protein production is mediated through a PARP-dependent pathway

Next, we studied the second important parameter of diabetic cardiomyopathy, ECM protein production. WT mice fed a galactose rich diet had significantly upregulated mRNA expression of FN when

compared to their WT controls (Fig. 3a). However, such galactose-induced effects were not evident in the PARP^{-/-} animals (Fig. 3a) suggesting a regulatory role of PARP in the expression of FN. It is of interest to note that in the PARP^{-/-} mice, the basal levels of FN mRNA were elevated compared to the WT controls animals (Fig. 3a). We have previously demonstrated that vasoactive factor ET-1 may regulate diabetes-induced FN production [10,11]. Such increase in ET-1 mRNA was also present in galactose-fed animals and was prevented in the PARP^{-/-} animals (Fig. 3a).

Parallel experiments in diabetic rat hearts showed a significant increase in the production of FN and ET-1mRNA (Fig. 3b). Inhibition of PARP through the daily administration of ABA in the diabetic animals completely prevented the diabetes-induced effects on these genes (Fig. 3b). Western blot analysis of FN showed similar patterns of expression between the treatment groups in the rat hearts as the mRNA results (data not shown).

Histological analyses of the heart tissues were done on both the mice and the rats. As with the molecular studies, hyperhexosemia in the WT mice and rats lead to areas of focal fibrosis (Fig. 3c) as demonstrated by trichrome staining. Inhibition of PARP prevented these hyperhexosemia-induced effects in the myocardium of both the mice and the rats (Fig. 3c).

3.3. PARP activation mediates hyperhexosemia-induced cardiac hypertrophy

Heart weight to body weight ratios were determined to assess myocardial hypertrophy. These ratios were significantly increased in the hyperhexosemic mice and rats compared to their respective controls (Figs. 4a and b). Interestingly, this hyperhexosemia-induced hypertrophy was not seen in the PARP^{-/-} mice fed galactose compared to its corresponding control and was significantly lowered in the diabetic rats treated with ABA compared to the diabetic rats indicating that PARP inhibition can at least in part prevent hyperhexosemia-induced cardiac hypertrophy *in vivo* (Figs. 4a and b).

3.4. PARP may regulate gene expression at the transcriptional level

At the chromosomal level, alteration of transcriptional coactivators may influence PARP-dependent gene expression. We investigated transcriptional co-activator p300, a HAT, and HDAC activity. The WT mice showed increased cardiac p300 transcript levels in animals given a high galactose diet compared to those fed normal rodent feed (Fig. 5a). As with FN and ET-1, the basal levels of p300 expression is significantly increased in comparison to the WT controls. The exact reason for such changes is not clear. The possibility that other co-regulatory mechanisms may affect this process cannot be excluded. However, the PARP^{-/-} mice fed a galactose enriched diet expressed p300 levels similar to that of the WT control mice (Fig. 5a). Similarly, in the rats, the hearts of the diabetic animals exhibited significantly increased levels p300 mRNA when compared to the control animals (Fig. 5b). ABA treatment prevented this hyperglycemia-induced increase of p300 mRNA (Fig. 5b).

As histone acetylation of p300 may be balanced by HDACs, we investigated HDAC activity. We found that in both the galactose-fed WT mice and the diabetic rat heart levels of deacetylated lysine were elevated compared to the WT mice and control rats, respectively (Figs. 5c and d). Interestingly, PARP inhibition had no effect on these hyperhexosemia-induced effects in either the PARP^{-/-} mice or the diabetic rats (Figs. 5c and d).

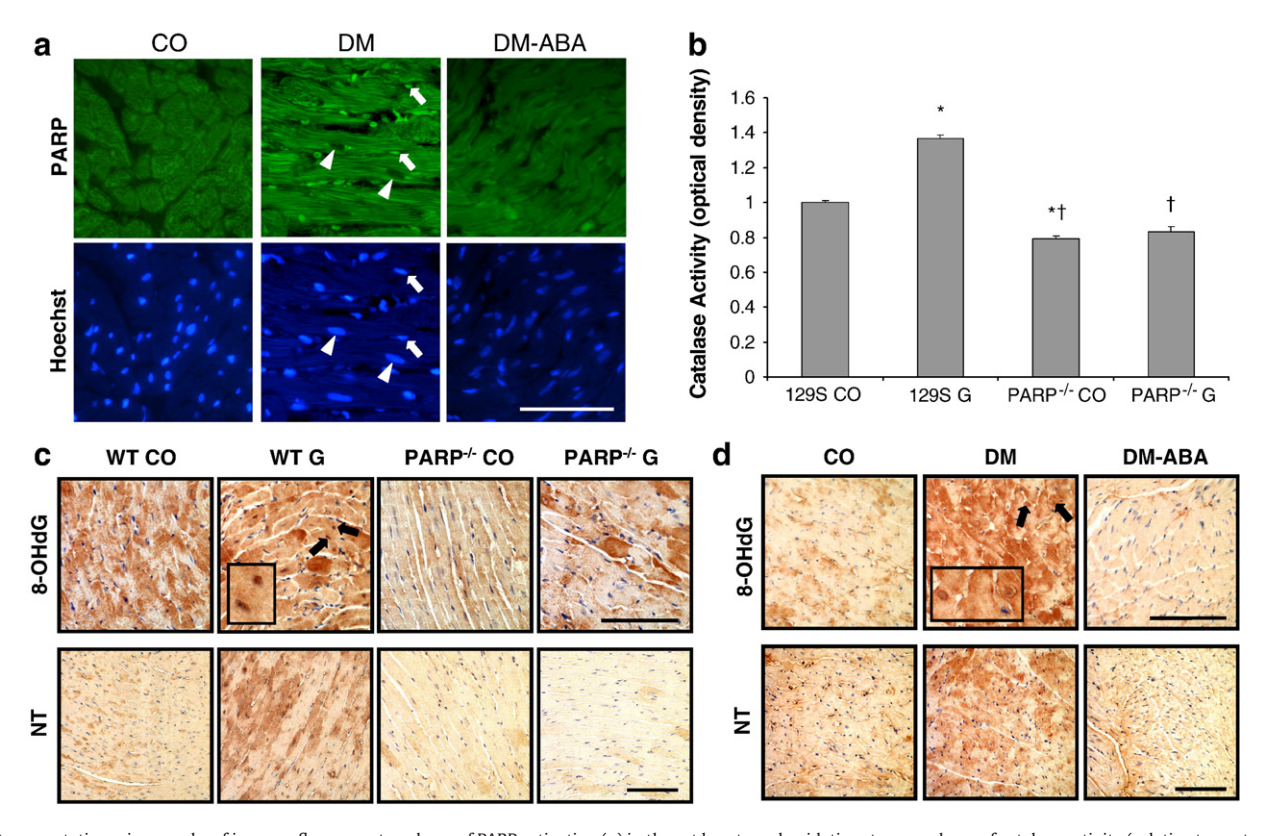


Fig. 2. Representative micrographs of immunofluorescent analyses of PARP activation (a) in the rat hearts and oxidative stress analyses of catalase activity (relative to control) in the mice (b) as well as immunohistochemical analyses of oxidative stress markers 8-OHdG and NT in mice (c) and rat (d) heart tissues. Hyperhexosemia-induced increased PARP activation and oxidative stress which is prevented with PARP inhibition [n=3 per group; arrows = positive nuclei, arrowheads = marker negative nuclei, insets show higher magnification (150×); bars represents 20 µm, magnification is the same for all micrographs in each panel; *p<0.05 compared to WT CO, p<0.05 compared to WT G; WT = wild type, PARP-p<0.05 represents 20 µm, magnification diet, DM = diabetes mellitus, ABA = 3-aminobenzamide, Hoechst = nuclear marker].

3.5. PARP inhibition in vitro produces similar effects as in vivo

To further verify our *in vivo* results, we investigated whether glucose causes similar effects in isolated heart cells. To test this, we isolated neonatal cardiomyocytes and exposed the cells to high levels of glucose. Twenty five mmol/L glucose caused cardiomyocte hypertrophy after 24 h as measured morphometrically (Fig. 6a). ABA was effective in blocking glucose-induced cellular hypertrophy (Fig. 6a). Interestingly, ABA reduced cardiomyocyte size in cells exposed to LG (Fig. 6a). A more potent PARP inhibitor was also utilized to ensure the specificity of the response. Sixteen µmol/L of ISO prevented high glucose-induced cardiomyocyte hypertrophy (Fig. 6a).

DNA damage was also determined using cultured neonatal cardiomyocytes. These cells were stained for phospho-H2A.X, a marker for double stranded DNA breakage [20]. High glucose treatment resulted in increased nuclear staining in these cells compared to the cells subjected to LG indicating increased double stranded DNA breaks (Fig. 6b). Interestingly, ABA and ISO treatment in both LG and HG environments yielded less nuclear positivity than that of the cardiomyocytes subjected only to a low glucose environment (Fig. 6b). These results indicate that PARP inhibition can prevent double stranded DNA breaks induced by hyperglycemia, possibly as a result of oxidative stress, ultimately resulting in the prevention of glucose-induced cellular damage.

3.6. HDACs may also influence glucose-induced gene expression through PARP in vitro

To further characterize whether ABA alters gene expression of ET-1 and FN as well as to determine the role of HDACs in this pathway we

used HUVECs. We have previously demonstrated that glucose causes PARP, p300, ET-1 and FN upregulation in these cells [10,17]. These cells were treated with HDAC inhibitor TSA. High glucose significantly upregulated the expression of PARP, p300 and FN mRNA (Fig. 7a) compared to normal glucose levels. This glucose-induced effect was prevented with TSA treatment (Fig. 7a). Additionally, PARP-dependent ET-1 and FN expression were also assessed in HUVECs. Twenty five mmol/L of glucose significantly upregulated these transcripts but this glucose-induced increase was prevented with PARP inhibition (Fig. 7b).

4. Discussion

The novelty of this study lies in the elucidation of a specific PARPmediated pathway in hyperhexosemia-induced structural alterations in the heart. Our findings in conjunction with the findings from the available literature demonstrate a significant role for PARP-dependent increase in oxidative stress in the pathogenesis of diabetic cardiomyopathy [27]. As well, our results from this and a previous study offer a novel regulatory mechanism for these PARP-mediated changes by transcriptional co-activator p300 [17]. These are consistent with previous findings indicating that PARP and p300 may interact to alter gene expression [8,28]. Downstream effects, such as PARP-dependent upregulation of vasoactive factor ET-1 and ECM protein FN along with cardiac hypertrophy can detrimentally impair the function of the heart. This investigation elucidates, for the first time, a novel mechanistic pathway for the action of PARP in diabetes-induced structural alterations of the heart. These findings complement studies which implicate PARP in hyperglycemia-induced functional modifications in the heart [27,29]. Soriano et al. found that PARP inhibition not

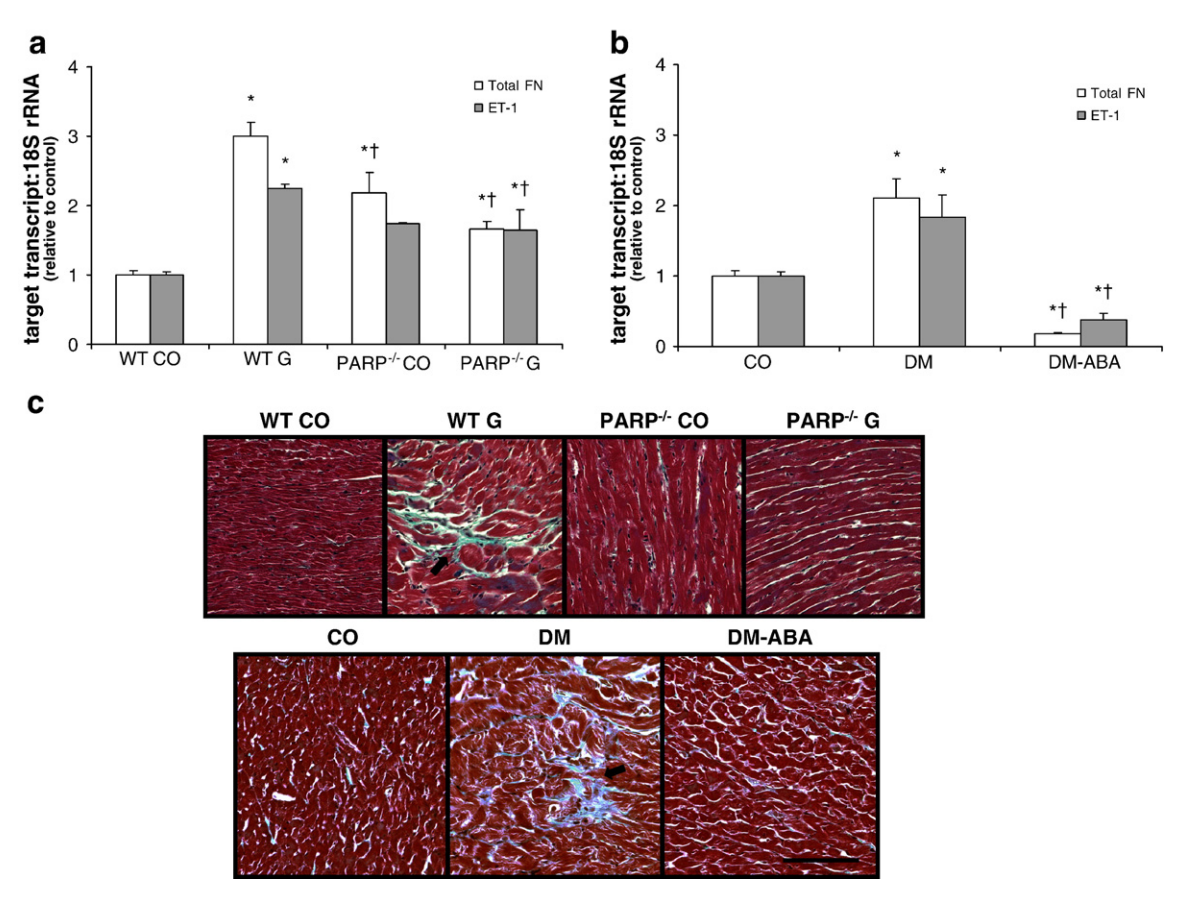


Fig. 3. Real time RT-PCR analysis of ECM protein FN and vasoactive factor ET-1 in mice (a) and rats (b) showing hyperhexosemia-induced upregulation of both genes. Trichrome stained heart sections (c) showed focal fibrosis in the hearts of mice (upper panel) and rats (lower panel). Hyperhexosemia-induced mRNA upregulation and focal fibrosis were prevented with PARP inhibition [n=5, mRNA is expressed as a ratio of target to 18S rRNA (relative to control); bar represents 20 μm; *p<0.05 compared to WT G (a) and DM (b); arrows indicate fibrotic areas; abbreviations similar to Fig. 2].

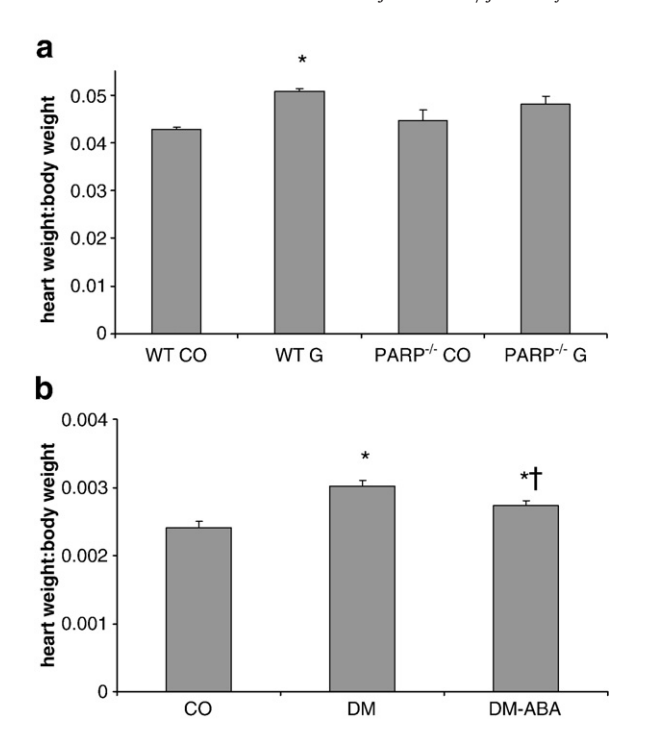


Fig. 4. Heart weight to body weight ratios of mice (a) and rats (b) showing hyperhexosemia-induced cardiac hypertrophy are prevented with PARP inhibition $[n=5; *p<0.05 \text{ compared to WT CO (a)} \text{ and CO (b)}, ^†p<0.05 \text{ compared to WT G (a)} \text{ and DM (b)}; abbreviations similar to Fig. 2].$

only prevented the development of endothelial dysfunction in 4 and 8 week old STZ-induced diabetic mice but also restored endothelium-dependent relaxant abilities in animals with already established

endothelial dysfunction [29]. Futhermore, Pacher et al. found that diabetes-induced depression of left ventricular systolic pressure and elevation of left ventricular end-diastolic pressure was prevented in diabetic mice and rats treated with PARP inhibitor PJ34 [27].

The usage of a galactose-induced model of chronic diabetic complications is well-established. Both biochemical and structural changes associated with these complications have been demonstrated using this model. In the heart, galactose feeding has been shown to elicit cardiac muscle contractile abnormalities due to the accumulation of polyols [14].

In the context of the present study, oxidative stress-induced DNA damage activates PARP. Several mechanisms may lead to oxidative stress in diabetes; increased superoxide anion generation at the mitochondrial level appears to be a key mechanism [30]. However, other possible pathways may include advanced glycation end products-mediated signaling as well as alterations in intracellular NADPH/NAD⁺ levels [30,31]. PARP activation, due to oxidative stress, plays a variety of roles in the cell; it can repair DNA damage, mediate gene expression and induce cell death [3,28,32]. This and previous studies have demonstrated a role for PARP activation in the retina, peripheral nerves, kidney and heart in diabetes [15,26]. The enzymatic activity of PARP may contribute to an overall increase in oxidative stress by creating a redox imbalance through its consumption of NAD+ [4]. As previously proposed, this may explain the overall reduction of oxidative stress in the hearts of the hyperhexosemic animals when PARP is inhibited and suggests that PARP activation may be a primary contributor to the increased levels of oxidative stress [27].

This notion is further strengthened upon analysis of double stranded DNA breakage. Previously, Du et al. found that 30 mM glucose increases DNA damage [33]. Our findings indicate that PARP inhibition may in fact be beneficial in circumstances of PARP overactivation and is in support of previously conducted research [26]. However, it is in contrast to other findings which suggest that

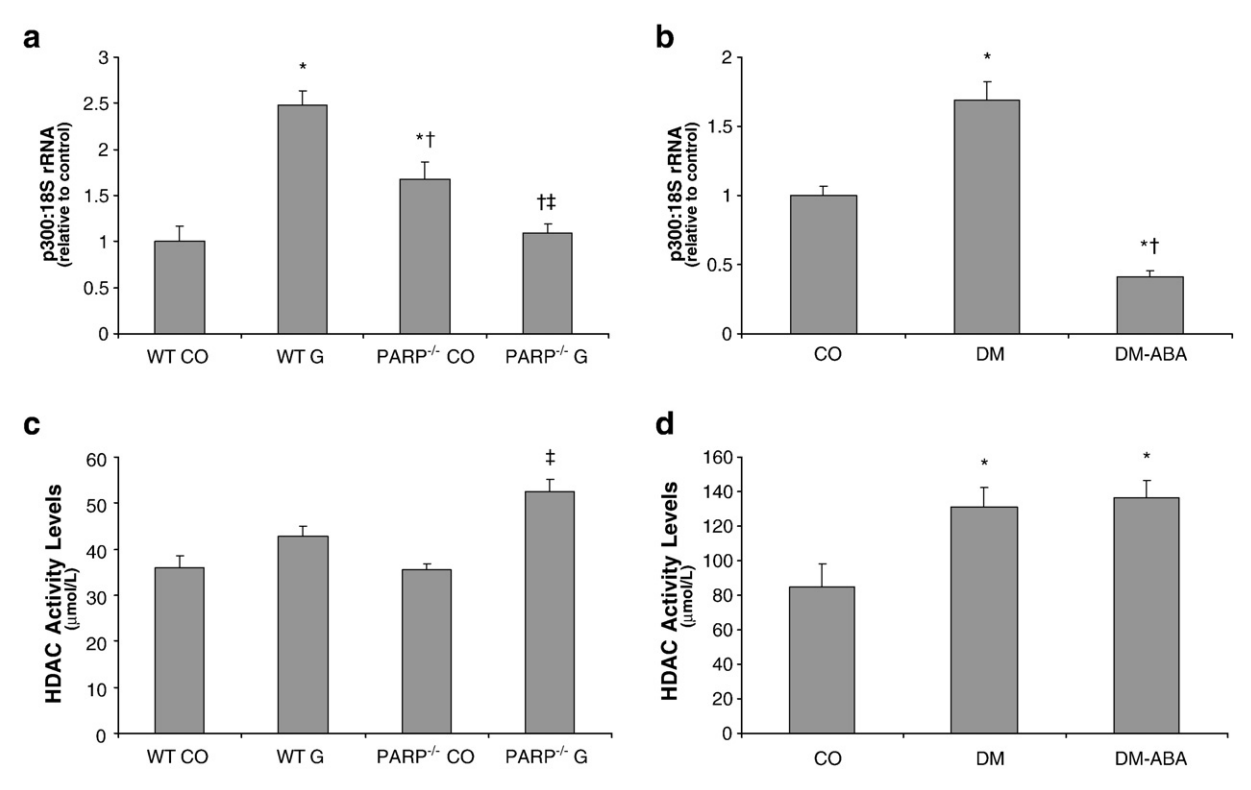


Fig. 5. Real time RT-PCR of p300 mRNA and HDAC activity in mice (a and c) and rats (b and d) showing hyperhexosemia-induced increased expression of p300 and HDAC activity levels. PARP inhibition prevented these hyperhexosemia-induced p300 mRNA levels but not HDAC induction [n=5, mRNA is expressed as a ratio of target to 18S rRNA (relative to control); HDAC activity is expressed as the absolute amount of deacetylated lysine/sample (μ mol/L); *p<0.05 compared to WT CO (a) and CO (b), †p<0.05 compared to WT G (a) and DM (b) and †p<0.05 compared to PARP^{-/-} CO (a); abbreviations similar to Fig. 2].

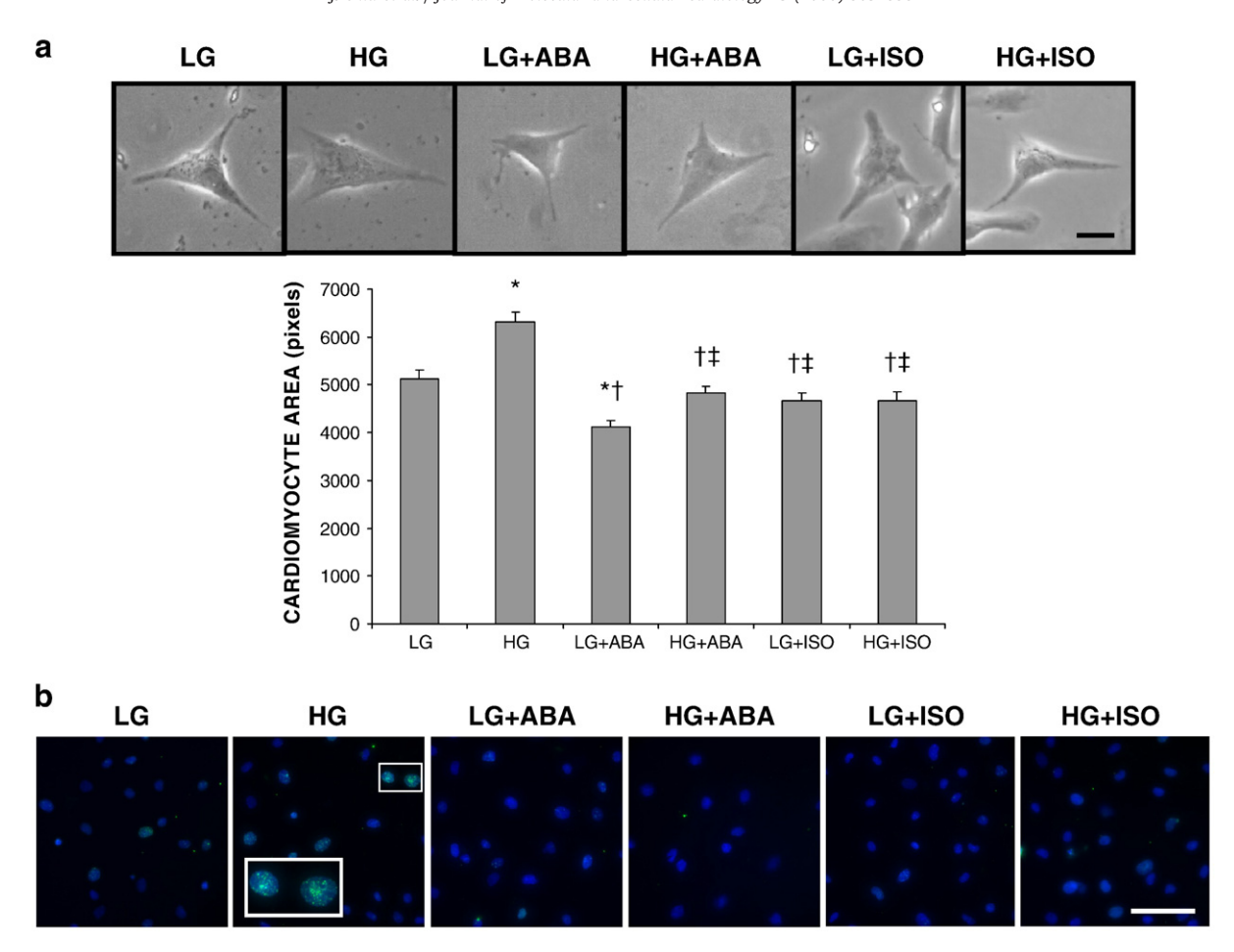
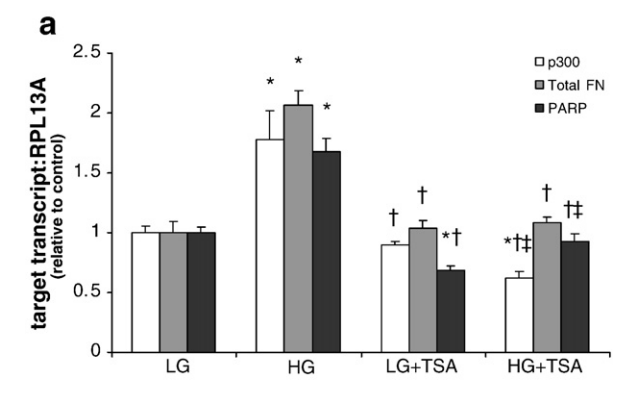


Fig. 6. Representative micrographs of neonatal cardiomyocytes and their morphometric analysis (a) and immunofluorescent staining of DNA damage by phospho-H2A.X (b) showing glucose-induced myocyte hypertrophy and DNA damage are normalized with PARP inhibitors ABA and ISO [bar in (a) represents 20 μ m; scale bar in (b) represents 50 μ m, insets show higher magnification (125×); *p<0.05 compared to LG, †p<0.05 compared to HG and †p<0.05 compared to LG+ABA; LG = 5 mmol/L glucose, HG = 25 mmol/L glucose, ABA = 3-aminobenzamide, ISO = 1,5-isoquinolinediol].

PARP inhibition increases double stranded DNA breaks [34]. This discrepancy may lie in the cause of the DNA damage, oxidative stressinduced versus ionizing radiation-induced and whether or not PARP is overactivated. These findings indicate that different mechanisms of DNA damage may lead to different tissue responses. Diabetic cardiomyopathy, due to hyperglycemia, is a slow chronic process while radiation may cause acute tissue injury. However, further investigation is necessary to elucidate the exact mechanism by which PARP inhibition may stimulate or prevent DNA strand breakage. One cannot exclude the possibility that other actions of ABA such as a scavenger of free radicals [35] may play a role in preventing this hyperglycemia-induced double stranded DNA damage seen in the cardiomyocytes and decreased staining positivity of oxidative stress markers 8-OHdG and NT in the rats. However, our studies included PARP-1^{-/-} mice which exhibited similar staining patterns of the aforementioned markers as the ABA-treated rats and treatments with ISO, a potent PARP inhibitor, yielded results that mirror our in vitro ABA studies. This further strengthens our notion that inhibition of PARP is the primary reason a reduction in hyperhexosemia-induced oxidative stress is seen rather than a confounding result due to the non-specific actions of ABA. In further support of the efficacy of ABA on preventing PARP inhibition, this compound was found to provide comparable degrees of restoration of endothelium-dependent relaxation capacities in diabetic blood vessels when compared to other more potent inhibitors of PARP [29]. In addition, ABA-treated blood vessels had NAD+ levels that were significantly elevated compared to diabetic controls while NADH levels were significantly lowered [29].

We have previously shown that p300 is upregulated in the heart and in the retina of diabetic animals and in endothelial cells exposed to HG levels [17]. We have also demonstrated that p300 regulates the expression of ECM protein FN in the context of diabetes [17], p300 directly interacts with the p65 subunit of NFkB to regulate the transcription of multiple genes [36]. In diabetic retinopathy, NFkB has been shown to be regulated by PARP possibly through p300 [37]. It has been reported that both PARP and p300 interact to form a complex which regulates gene expression by binding onto promoter regions [8]. Furthermore, it has been suggested that the presence of the PARP protein itself is what mediates its co-activator function on NFKB and not its DNA binding nor its enzymatic activity [38]. Our lab has shown that activation of transcription factors NFkB and AP-1 mediates the expression of FN in all target organs of diabetic complications [11]. In addition, PARP has been shown to regulate NFkB transcriptional activation in vivo and that this regulation is through p300 [8]. Our study showed that PARP inhibition attenuated the hyperhexosemiainduced upregulation of p300 in both rodent models and in vitro in HUVECs. We also found that hyperhexosemia-induced increased FN levels were reduced when PARP is inhibited, showing the same trends as p300. These findings suggest that PARP mediates its hyperhexosemia-induced transcriptional effects through p300 and may utilize other transcription factors, such as NFkB, to regulate hyperhexosemiainduced upregulation of FN. The possibility of the involvement of other transcriptional co-activators such as CREB binding protein and other transcription factors cannot be excluded and would require further investigation.



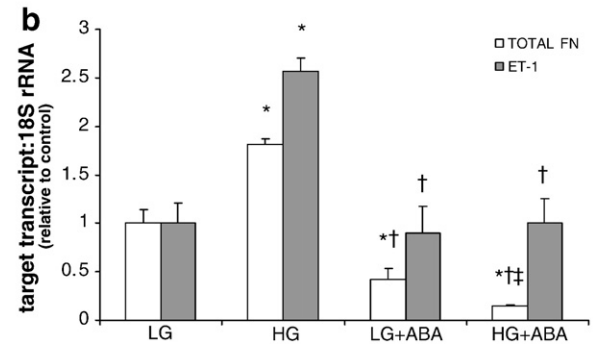


Fig. 7. Real time RT-PCR analyses of HUVECs showing hyperglycemia-induced increased PARP, p300 and FN mRNA were normalized with TSA treatment (a) and ABA treatment also prevented glucose-induced ET-1 and FN upregulation (b) [n=5, mRNA is expressed as a ratio of target to housekeeping gene (relative to control); *p<0.05 compared to LG, $^{\dagger}p$ <0.05 compared to HG and $^{\dagger}p$ <0.05 compared to LG+ABA or LG+TSA; TSA = trichostatin A, all other abbreviations similar to Fig. 6].

The action of HATs, such as p300, are counteracted by HDACs [39]. It is of interest to note that in our studies HDAC activity levels were increased in the diabetic rats and the WT galactose-fed mice. This was unexpected since there was increased gene expression of FN and ET-1 seen in these animals. However, this finding suggests that HDACs may either be attempting to counteract the elevated levels of HATs such as p300 through increased deacetylation of lysine residues in hyperhexosemic conditions even with PARP inhibition or that HDACs may play a role in this pathway upstream of PARP and p300. These notions are strengthened upon the treatment of HUVECs with HDAC inhibitor TSA which prevented the glucose-induced upregulation of PARP, p300 and FN mRNA. This signifies a more complex regulatory relationship between HATs and HDACs. However, the exact role of HDACs in the hyperhexosemic heart requires further investigation.

The finding that PARP activity is regulated through transcriptional co-activator(s), possibly by histone acetylation, is very interesting and provides insight into how PARP may exert its transcriptional effects. Furthermore, the finding that the relationship between HATs and HDACs may not be as simple as a balance suggests that a more complex interplay exists between the two molecules when regulating chromatin relaxation and gene expression. Such epigenetic regulation of gene expression has not been adequately explored in the context of diabetic cardiomyopathy and in other chronic diabetic complications.

Acknowledgments

The authors of this study would like to acknowledge the Canadian Diabetes Association, Canadian Institute of Health Research and the Heart and Stroke Foundation of Ontario (HSFO) for their funding support. Jane Chiu was supported by the HSFO program in heart

failure. We would also like to thank Dr. Zia A. Khan, Department of Pathology, for his invaluable suggestions and comments.

References

- Saito F, Kawaguchi M, Izumida J, Asakura T, Maehara K, Maruyama Y. Alteration in haemodynamics and pathological changes in the cardiovascular system during the development of Type 2 diabetes mellitus in OLETF rats. Diabetologia 2003;46 (8):1161–9.
- [2] Fein FS. Diabetic cardiomyopathy. Diabetes Care 1990;13(11):1169-79.
- [3] Gaal JC, Pearson CK. Eukaryotic nuclear ADP-ribosylation reactions. Biochem J 1985;230(1):1–18.
- [4] Pieper AA, Brat DJ, Krug DK, Watkins CC, Gupta A, Blackshaw S, et al. Poly(ADPribose) polymerase-deficient mice are protected from streptozotocin-induced diabetes. Proc Natl Acad Sci U S A 1999;96(6):3059–64.
- [5] Yang Z, Zingarelli B, Szabo C. Effect of genetic disruption of poly (ADP-ribose) synthetase on delayed production of inflammatory mediators and delayed necrosis during myocardial ischemia-reperfusion injury. Shock 2000;13(1):60–6.
- [6] Chan HM, La Thangue NB. p300/CBP proteins: HATs for transcriptional bridges and scaffolds. J Cell Sci 2001;114(Pt 13):2363–73.
- [7] Lee JW, Lee YC, Na SY, Jung DJ, Lee SK. Transcriptional coregulators of the nuclear receptor superfamily: coactivators and corepressors. Cell Mol Life Sci 2001;58 (2):289–97.
- [8] Hassa PO, Haenni SS, Buerki C, Meier NI, Lane WS, Owen H, et al. Acetylation of poly(ADP-ribose) polymerase-1 by p300/CREB-binding protein regulates coactivation of NF-kappaB-dependent transcription. J Biol Chem 2005;280 (49):40450-64.
- [9] Yamada KM. Cell surface interactions with extracellular materials. Annu Rev Biochem 1983;52:761–99.
- [10] Chen S, Mukherjee S, Chakraborty C, Chakrabarti S. High glucose-induced, endothelin-dependent fibronectin synthesis is mediated via NF-kappa B and AP-1. Am J Physiol Cell Physiol 2003;284(2):C263–72.
- [11] Chen S, Khan ZA, Cukiernik M, Chakrabarti S. Differential activation of NF-kappa B and AP-1 in increased fibronectin synthesis in target organs of diabetic complications. Am J Physiol Endocrinol Metab 2003;284(6):E1089–97.
- [12] Chen S, Evans T, Deng D, Cukiernik M, Chakrabarti S. Hyperhexosemia induced functional and structural changes in the kidneys: role of endothelins. Nephron 2002;90(1):86–94.
- [13] Kern TS, Engerman RL. A mouse model of diabetic retinopathy. Arch Ophthalmol 1996:114(8):986–90.
- [14] Cotter MA, Cameron NE, Robertson S. Polyol pathway-mediated changes in cardiac muscle contractile properties: studies in streptozotocin-diabetic and galactosefed rats. Exp Physiol 1992;77(6):829–38.
- [15] Obrosova IG, Li F, Abatan OI, Forsell MA, Komjati K, Pacher P, et al. Role of poly (ADP-ribose) polymerase activation in diabetic neuropathy. Diabetes 2004;53 (3):711–20.
- [16] Khan ZA, Cukiernik M, Gonder JR, Chakrabarti S. Oncofetal fibronectin in diabetic retinopathy. Invest Ophthalmol Vis Sci 2004;45(1):287–95.
- [17] Kaur H, Chen S, Xin X, Chiu J, Khan ZA, Chakrabarti S. Diabetes-induced extracellular matrix protein expression is mediated by transcription coactivator p300. Diabetes 2006;55(11):3104–11.
- [18] Floyd RA, Watson JJ, Wong PK, Altmiller DH, Rickard RC. Hydroxyl free radical adduct of deoxyguanosine: sensitive detection and mechanisms of formation. Free Radic Res Commun 1986;1(3):163–72.
- [19] Beckman JS, Koppenol WH. Nitric oxide, superoxide, and peroxynitrite: the good, the bad, and ugly. Am J Physiol 1996;271(5 Pt 1):C1424–37.
- [20] Redon C, Pilch D, Rogakou E, Sedelnikova O, Newrock K, Bonner W. Histone H2A variants H2AX and H2AZ. Curr Opin Genet Dev 2002;12(2):162–9.
- [21] Dignam JD, Lebovitz RM, Roeder RG. Accurate transcription initiation by RNA polymerase II in a soluble extract from isolated mammalian nuclei. Nucleic Acids Res 1983;11(5):1475–89.
- [22] Gan XT, Chakrabarti S, Karmazyn M. Increased endothelin-1 and endothelin receptor expression in myocytes of ischemic and reperfused rat hearts and ventricular myocytes exposed to ischemic conditions and its inhibition by nitric oxide generation. Can J Physiol Pharmacol 2003;81(2):105–13.
- [23] Dyck JR, Maddaford TG, Pierce GN, Fliegel L. Induction of expression of the sodium-hydrogen exchanger in rat myocardium. Cardiovasc Res 1995;29(2):203–8.
- [24] Farhangkhoee H, Khan ZA, Mukherjee S, Cukiernik M, Barbin YP, Karmazyn M, et al. Heme oxygenase in diabetes-induced oxidative stress in the heart. J Mol Cell Cardiol 2003;35(12):1439–48.
- [25] Mogal A, Abdulkadir SA. Effects of histone deacetlase inhibitor (HDACi); Trichostatin-A (TSA) on the expression of housekeeping genes. Mol Cell Probes 2006;20(2):81-6.
- [26] Garcia SF, Virag L, Jagtap P, Szabo E, Mabley JG, Liaudet L, et al. Diabetic endothelial dysfunction: the role of poly(ADP-ribose) polymerase activation. Nat Med 2001;7 (1):108–13
- [27] Pacher P, Liaudet L, Soriano FG, Mabley JG, Szabo E, Szabo C. The role of poly(ADPribose) polymerase activation in the development of myocardial and endothelial dysfunction in diabetes. Diabetes 2002;51(2):514–21.
- [28] Hassa PO, Buerki C, Lombardi C, Imhof R, Hottiger MO. Transcriptional coactivation of nuclear factor-kappaB-dependent gene expression by p300 is regulated by poly (ADP)-ribose polymerase-1. J Biol Chem 2003;278(46):45145–53.
- [29] Soriano FG, Pacher P, Mabley J, Liaudet L, Szabo C. Rapid reversal of the diabetic endothelial dysfunction by pharmacological inhibition of poly(ADP-ribose) polymerase. Circ Res 2001;89(8):684–91.

- [30] Brownlee M. Biochemistry and molecular cell biology of diabetic complications. Nature 2001;414:813–20.
- Ceriello A. New insights on oxidative stress and diabetic complications may lead to
- a "causal" antioxidant therapy. Diabetes Care 2003;26:1589–96.

 [32] Masson M, Rolli V, Dantzer F, Trucco C, Schreiber V, Fribourg S, et al. Poly(ADPribose) polymerase: structure-function relationship. Biochimie 1995;77(6): 456-61
- [33] Du X, Matsumura T, Edelstein D, Rossetti L, Zsengeller Z, Szabo C, et al. Inhibition of GAPDH activity by poly(ADP-ribose) polymerase activates three major pathways of hyperglycemic damage in endothelial cells. J Clin Invest 2003;112(7):
- [34] Veuger SJ, Curtin NJ, Smith GC, Durkacz BW. Effects of novel inhibitors of poly (ADP-ribose) polymerase-1 and the DNA-dependent protein kinase on enzyme activities and DNA repair. Oncogene 2004;23(44):7322-9.
- [35] Wilson GL, Patton NJ, McCord JM, Mullins DW, Mossman BT. Mechanisms of streptozotocin- and alloxan-induced damage in rat B cells. Diabetologia 1984;27
- [36] Gerritsen ME, Williams AJ, Neish AS, Moore S, Shi Y, Collins T. CREB-binding protein/p300 are transcriptional coactivators of p65. Proc Natl Acad Sci U S A 1997:94(7):2927-32.
- Zheng L, Szabo C, Kern TS. Poly(ADP-ribose) polymerase is involved in the development of diabetic retinopathy via regulation of nuclear factor-kappaB. Diabetes 2004:53(11):2960-7.
- [38] Hassa PO, Covic M, Hasan S, Imhof R, Hottiger MO. The enzymatic and DNA binding activity of PARP-1 are not required for NF-kappa B coactivator function. | Biol Chem 2001;276(49):45588–97.
- Sadoul K, Boyault C, Pabion M, Khochbin S. Regulation of protein turnover by acetyltransferases and deacetylases. Biochimie 2008;90(2):306–12.